Preventive Veterinary Medicine, 11 (1991) 185–200
Elsevier Science Publishers B.V., Amsterdam

Interpreting vegetation indices

Ray D. Jackson[a] and Alfredo R. Huete[b]
[a]*USDA-ARS, US Water Conservation Laboratory, Phoenix, AZ 85040, USA*
[b]*Department of Soil and Water Science, University of Arizona, Tucson, AZ 85721, USA*

ABSTRACT

Jackson, R.D. and Huete, A.R., 1991. Interpreting vegetation indices. *Prev. Vet. Med.*, 11: 185–200.

Remotely sensed spectral vegetation indices are widely used and have benefited numerous disciplines interested in the assessment of biomass, water use, plant stress, plant health and crop production. The successful use of these indices requires knowledge of the units of the input variables used to form the indices, and an understanding of the manner in which the external environment and the architectural aspects of a vegetation canopy influence and alter the computed index values. Although vegetation indices were developed to extract the plant signal only, the soil background, moisture condition, solar zenith angle, view angle, as well as the atmosphere, alter the index values in complex ways. The nature of these problems are explored both in an empirical and in a theoretical sense, and suggestions are offered for the effective use and interpretation of vegetation indices.

INTRODUCTION

A primary goal of many remote sensing projects is to characterize the type, amount and condition of vegetation present within a scene. The amount of light reflected from a surface is determined by the amount and composition of solar irradiance that strikes the surface, and the reflectance properties of the surface. Because solar irradiance varies with time and atmospheric conditions, a simple measure of light reflected from a surface is not sufficient to characterize the surface in a repeatable manner. This problem can be circumvented somewhat by combining data from two or more spectral bands to form what is commonly known as a vegetation index (VI). A VI can be calculated by ratioing, differencing, ratioing differences and sums, and by forming linear combinations of spectral band data. VI are intended to enhance the vegetation signal, while minimizing solar irradiance and soil background effects.

The ubiquitous use of VI would suggest that they are calculated in a uniform manner, and that they are comparable over time and location. Unfortunately, this is not the case. VI can be calculated from sensor voltage outputs (V), radiance values (L), reflectance values (ρ) and satellite digital numbers (DN). Each is correct, but each will yield a different VI value for the same

© 1991 Elsevier Science Publishers B.V. All rights reserved 0167-5877/91/$03.50

surface conditions. View and solar angles affect data from each spectral band differently, and thus may affect VI values. Soil background exerts a major influence on VI. VI calculated from data obtained from aircraft- or spacecraft-based sensors are affected by the intervening atmosphere. VI calculated from data obtained over the same target, but with different instruments, may not be the same because of detector and filter characteristics of the instruments. It is the purpose of this report to demonstrate the magnitude of differences that can occur, and to provide suggestions for the effective use and interpretation of VI.

THE CONCEPT OF VI

When light strikes a surface, part is reflected, part is transmitted and the remainder is absorbed. The relative amounts of reflected, transmitted and absorbed light are a function of the surface and vary with the wavelength of the light. For example, the majority of light striking soils is either reflected or absorbed, with very little being transmitted and relatively little change with wavelength. With vegetation, however, most of the light in the near-infrared (NIR) wavelengths is transmitted and reflected, with little absorbed, in contrast to the visible wavelengths where absorption is predominant, with some reflected and little transmitted.

Reflectance spectra for bare dry soil, bare wet soil and a full-cover wheat canopy are depicted in Fig. 1. The vertical dashed lines labeled 'red' and 'near-infrared' delineate the wavelength intervals representative of Bands 3 and 4 of the Thematic Mapper (TM) on LANDSATS 4 and 5, and Bands 2 and 3 of the high resolution visible (HRV) sensors on the French satellites SPOT 1 and 2. Horizontal solid lines labeled A–F indicate the average reflectance within the waveband for the soil and wheat targets. If a wheat field is to be monitored, early in the season only bare soil will be observed by the sensor.

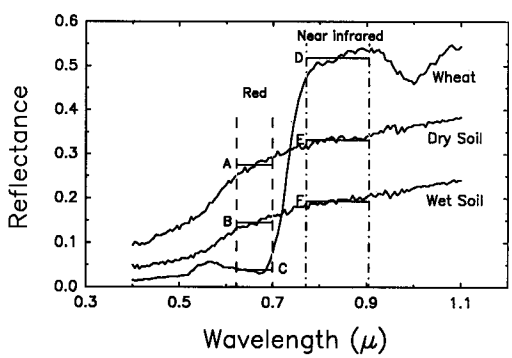

Fig. 1. Reflectance spectra for wheat, dry bare soil, and wet bare soil. Vertical dashed lines indicate the approximate band widths of the red and NIR bands of the LANDSAT TM.

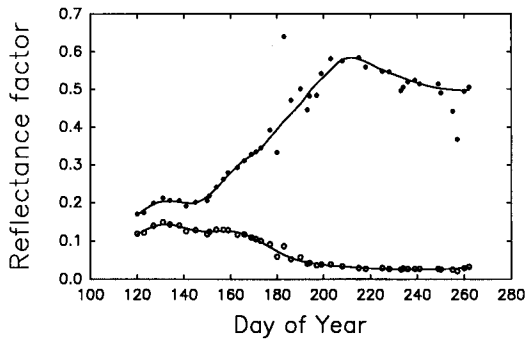

Fig. 2. Reflectance factor data for the red (open circles) and NIR bands (solid circles) measured over cotton. The solid lines represent smoothed data.

As the plants develop, the output in the red band decreases from A (if the soil is dry) or B (if wet), reaching C when the plants fully cover the soil. In the NIR, the output increases from Point E (if the soil is dry) or F (if wet), toward Point D. In general, the wavebands used to calculate VI are chosen such that one decreases and the other increases with increasing vegetation cover.

Seasonal trends of NIR and red reflectances for cotton are shown in Fig. 2. The reflectance measurements were made with a hand-held radiometer with band filters similar to those in Bands 2 and 3 of the HRV sensors aboard SPOT-1. The field was subirrigated, thus the soil surface remained essentially dry throughout the season. In Fig. 2, the red reflectance decreased and the NIR increased as the cotton plants grew and covered the soil. The solid line drawn through the points for both bands represent smoothed data that will be used in a subsequent graph.

CLASSES OF VI

There are two general classes of VI: ratios and linear combinations, both of which exploit the surface-dependent and/or wavelength-dependent features of the data shown in Figs. 1 and 2. Ratio VI may be the simple ratio of any two spectral bands, or the ratio of sums, differences or products of any number of bands. Linear combinations are orthogonal sets of n linear equations calculated using data from n spectral bands.

Ratios

The ratio vegetation index (RVI), formed by dividing the NIR radiance by the red radiance, was probably the first index to be defined and is the most commonly used. Tucker (1979) reported that Jordan (1969) used a radiance

ratio of 0.800/0.675 μm, measured at the forest floor, to derive a leaf area index for a forest canopy. In equation form, the RVI is

$$\mathrm{RVI}=\frac{\mathrm{NIR}}{\mathrm{red}} \tag{1}$$

RVI values for the data shown in Fig. 1 are 12.9 for wheat, 1.21 for bare dry soil and 1.33 for bare wet soil. For the cotton data shown in Fig. 2, the RVI was 1.43 on Day 130 (bare soil) and 20.2 on Day 225 (near-maximum green vegetation).

For dense green vegetation, the amount of red light reflected from the canopy is very small (open circles, Fig. 2). As can be seen in eqn. (1), as red band reflectance approaches zero, the ratio increases without bound. Thus, the amount of reflected red light must be measured with considerable accuracy if reasonable values of the ratio are to be expected. If the red band is measured with sufficient precision, the RVI is quite sensitive to vegetation changes during the time of peak growth. It is not very sensitive when the vegetative cover is sparse.

Deering (1978) found that the low dynamic range of the NIR/red ratio over sparse vegetation could be enhanced by ratioing the difference between the NIR and the red bands to the sum of the two bands. This VI was subsequently named the normalized difference vegetation index (NDVI). Thus

$$\mathrm{NDVI}=\frac{\mathrm{NIR}-\mathrm{red}}{\mathrm{NIR}+\mathrm{red}} \tag{2}$$

The upper bound of the NDVI approaches one, while the lower bound is usually close to zero. The lower bound may be slightly positive or slightly negative, depending on sensor characteristics and the units of the input variables (volts, radiance, reflectance, digital numbers, etc.). NDVI values for the wheat data in Fig. 1 are 0.86, 0.09 and 0.14 for wheat, dry soil and wet soil, respectively. NDVI for cotton (Fig. 2) are 0.18 and 0.96 for Days of Year 130 and 225, respectively.

The relative sensitivity of the NDVI and the RVI to vegetation density is demonstrated in Fig. 3. The values used for the lines were calculated from the smoothed data in Fig. 2 and normalized to range from zero to one. The normalization was required to facilitate comparison of the two indices. When plotted in this manner, it is evident that the NDVI (dashed line) is more sensitive to sparse vegetation densities than is the RVI, but is less sensitive to high vegetation densities.

From the mathematical point of view, these two indices are functionally equivalent and thus contain the same information. Perry and Lautenschlager (1984) addressed this point and showed that one index can be readily trans-

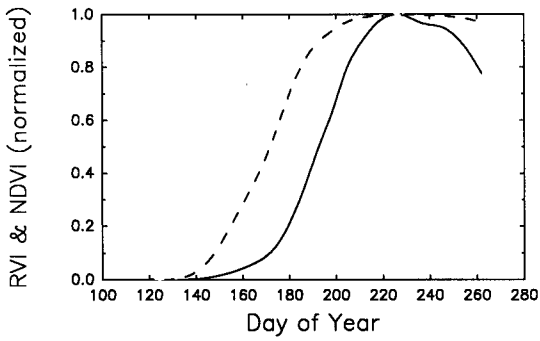

Fig. 3. NDVI (dashed line) and RVI (solid line) values calculated from the smoothed data of Fig. 2 and normalized to one to facilitate comparison.

formed into the other. Dividing both the numerator and the denominator of eqn. (2) by 'red', we have

$$\mathrm{NDVI}=\frac{\mathrm{RVI}-1}{\mathrm{RVI}+1} \tag{3}$$

A prime reason for using mathematical transformations is to improve the interpretation and visualization of the included information. Consider the period from Day 120 to 180 of Fig. 3. The normalized values of NDVI and RVI increased from 0 to about 0.8, and from 0 to about 0.2, respectively, and thus it is graphically easier to assess vegetation amounts with the NDVI than the RVI at low vegetation densities. However, after about Day 200, the NDVI graph is essentially flat, showing little visual change as the season progresses. The RVI graph increases and then decreases during this period, with a discernible visual change.

Linear combinations

VI, which are not functionally equivalent to ratios, can also be calculated from linear combinations of two or more spectral bands. A graphical example, using red and NIR bands, is depicted in Fig. 4. Point A in Fig. 4 corresponds to the values of red and NIR reflectances of the dry soil shown in Fig. 1. Point B corresponds to the reflectance values for the wet soil and Point C corresponds to vegetation. Thus, values of red and NIR data pairs representing any soil water content for bare soils would fall on the line connecting Points A and B of Fig. 4. Point C represents full vegetative cover in red–NIR space. As vegetation emerges from the soil, a red–NIR data pair would move toward Point C, keeping within the bounds indicated by the dotted lines connecting Points B–C and A–C. The shape formed by the dotted and solid lines is that of a 'tasseled cap', as first noted by Kauth and Thomas (1976). Point D rep-

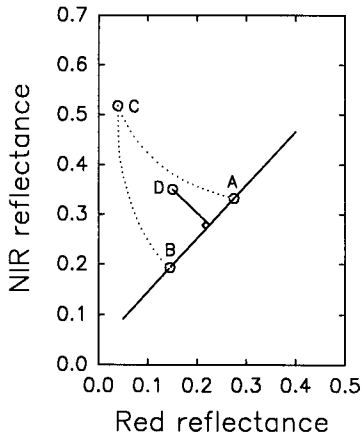

Fig. 4. Graphical representation of the 'tasseled cap' and the PVI.

resents intermediate vegetative growth with the soil at an intermediate water content. The perpendicular distance from Point D to the line A–B represents the perpendicular vegetation index (PVI) of Richardson and Wiegand (1977).

Kauth and Thomas (1976) applied the Gram–Schmidt technique (Freiberger, 1960) and, later, principle components analysis, to obtain four orthogonal linear combination indices (LCI) of the four LANDSAT multi spectral scanner (MSS) bands. Any index of this type can be written in the form

$$\mathrm{LCI} = \sum_{i=1}^{n} a_i X_i \tag{4}$$

where a is a coefficient, X is the band data, n is the number of bands and i is the respective band number.

Kauth and Thomas selected clusters of pixels identified as soil and other clusters identified as vegetation, and calculated unit vectors that form the coefficients of four indices: brightness (BR), greenness (GN), yellowness (YE) and nonsuch (NS). Their three-dimensional (3D) scatter plots of BR-, GN- and YE-transformed data resembled a 3D tasseled cap, the name they applied to their spectral–temporal description of agricultural crops. Basically, brightness represented a vector depicting the magnitude of reflected energy, particularly that of soils (soil line), greenness represented an orthogonal plane containing all of the vegetation information, while yellowness formed a plane orthogonal to both soils and vegetation. Yellowness has been related to atmospheric haze and senescent vegetation. Nonsuch contains most of the noise in the data (Lambeck et al., 1978; Kauth et al., 1979). Jackson (1983) reviewed the Kauth–Thomas procedure and presented a detailed ex-

ample of the calculation of four indices using the Gram–Schmidt technique on data for four bands similar to LANDSAT MSS Bands 4–7. Figure 4 shows a two-dimensional representation of the tasseled cap.

Concurrent with the development of the tasseled cap, Richardson and Wiegand (1977) proposed a PVI that utilized the red and NIR MSS bands of LANDSAT. This two-dimensional index required the specification of a soil line, with the index being the perpendicular distance from this line to the vegetation point. The PVI is the simplest linear combination index to calculate. An example of a PVI can be generated from data shown in Fig. 4. The coordinates for Points A and B are used to calculate a line passing through the two points. Next, a line perpendicular to the soil line that passes through any vegetation point, say Point D, is calculated. The distance from Point D to the intersection of the two orthogonal lines is the PVI. A detailed discussion of the algebraic basis for the PVI calculation was given by Jackson et al. (1980).

CALCULATING VI WITH DIFFERENT INPUT VARIABLES

VI can be calculated using raw detector output voltages (V) or processed data such as reflectances (ρ), radiances (L) or digital number (DN). This is an obvious, but sometimes overlooked factor when values of VI are compared. Essentially, all satellite data are reported in digital numbers (these are integers that generally range from 0 to 255), whereas ground-based radiometer data are usually first recorded as voltage outputs.

Transforming raw data into radiance requires knowledge of the calibration factors for each band on each instrument. Reflectance values can be calculated from either voltage output or radiance if a calibrated reference panel is also measured. Calculation of surface reflectance factors from satellite data requires the conversion of digital numbers to radiance, then the use of a radiative transfer model to account for atmospheric scattering and absorption.

The above discussion becomes evident when expressed in equation form. Thus, the RVI can be calculated from a simple voltage ratio

$$\mathrm{RVI}=\frac{V_{\mathrm{nir}}}{V_{\mathrm{red}}} \tag{5}$$

or from a radiance ratio

$$\mathrm{RVI}=\frac{L_{\mathrm{nir}}}{L_{\mathrm{red}}}=\frac{V_{\mathrm{nir}}C_{\mathrm{nir}}}{V_{\mathrm{red}}C_{\mathrm{red}}} \tag{6}$$

or from a reflectance ratio

$$\mathrm{RVI}=\frac{\rho_{\mathrm{nir}}(\mathrm{target})}{\rho_{\mathrm{red}}(\mathrm{target})}=\frac{[V_{\mathrm{nir}}(\mathrm{target})/V_{\mathrm{nir}}(\mathrm{panel})]\rho_{\mathrm{nir}}(\mathrm{panel})}{[V_{\mathrm{red}}(\mathrm{target})/V_{\mathrm{red}}(\mathrm{panel})]\rho_{\mathrm{red}}(\mathrm{panel})} \tag{7}$$

Unless the calibration coefficients (C) for the two bands are equal (this is seldom the case), it is obvious that eqns. (5) and (6) will yield different values of RVI. Equation (7) does not require knowledge of C values, but does require the reference panel calibration factors ρ_λ(panel).

Equations (5), (6) and (7) are most useful for ground-based instruments. For satellite data, the RVI can be calculated from a simple ratio of digital numbers, i.e.

$$\mathrm{RVI}=\frac{\mathrm{DN}_{\mathrm{nir}}}{\mathrm{DN}_{\mathrm{red}}} \tag{8}$$

which does not account for sensor calibration or atmospheric effects. Price (1987) presented a detailed discussion concerning how the calibration factors and other sensor characteristics of different satellites affect the resulting values of VI.

To obtain values of surface reflectance from digital numbers, the sensor calibration constants must be known, and the optical depth of the atmosphere must be measured at the time of data acquisition and used in a radiative transfer model. With these data, the RVI can be calculated from the equation

$$\mathrm{RVI}=\frac{\alpha_{\mathrm{nir}}E_{\mathrm{nir}}\mathrm{DN}_{\mathrm{nir}}C_{\mathrm{nir}}+\beta_{\mathrm{nir}}}{\alpha_{\mathrm{red}}E_{\mathrm{red}}\mathrm{DN}_{\mathrm{red}}C_{\mathrm{red}}+\beta_{\mathrm{red}}} \tag{9}$$

where α and β are constants obtained from a radiative transfer code, E is a factor that includes the exoatmospheric irradiance in the waveband and the solar zenith angle at the time of acquisition (Moran et al., 1990). It is apparent that the calculation of surface reflectance from satellite data requires data that are usually not readily available.

Although the above equations yield the RVI, all VI would be affected by the use of different input data.

COMPARISON OF VI USING DATA FROM DIFFERENT SENSORS

It is frequently desirable to compare the same VI over time and space using data from different sensors. A case in point is experiments in which ground-based data are compared with aircraft- and satellite-based data. Care must be exercised in making such comparisons because the band-response functions for each instrument are different, the fields of view are usually different and VI can be calculated using either raw or transformed data. The literature is replete with relationships between various VI and biomass (or leaf area index) that were developed using data from hand-held or boom-mounted radiometers. A comparison of these relationships with satellite-derived VI should be made with caution. It is necessary to ascertain how the VI were calculated, what sensor was used, and what the environmental and atmospheric conditions were at the time of measurement.

The detectors and filters that are used to measure light within a particular wavelength interval are unique to each instrument. The response function for a particular band is a combination of the wavelength-dependent detector and filter response. For example, LANDSAT-TM, SPOT-HRV and National Oceanic and Atmospheric Administration (NOAA)-advanced very high resolution radiometer (AVHRR) sensors each have a red and a NIR band, and the response of each is different for both bands (Fig. 5). In Fig. 5, the dashed lines refer to the LANDSAT-TM response, the dash–dot–dash lines refer to SPOT-HRV and the dotted lines to NOAA-AVHRR. Solid lines in the figure refer to wheat and bare soil spectra (extracts of spectra shown in Fig. 1). The response functions for LANDSAT-TM and SPOT-HRV are similar, but the NOAA-AVHRR extends over a wider wavelength interval and is of a somewhat different shape.

The effect of the different response functions on VI values can be assessed by calculating average reflectance factors for each band and each instrument. This was accomplished by integrating the product of the response function and the spectra values over the wavelengths for which the response functions were non-zero, and dividing by the integral of the response function over the same wavelength interval (Slater, 1980). The results are given in Table 1, along with calculated VI.

For this theoretical example, wheat reflectance values were similar for the

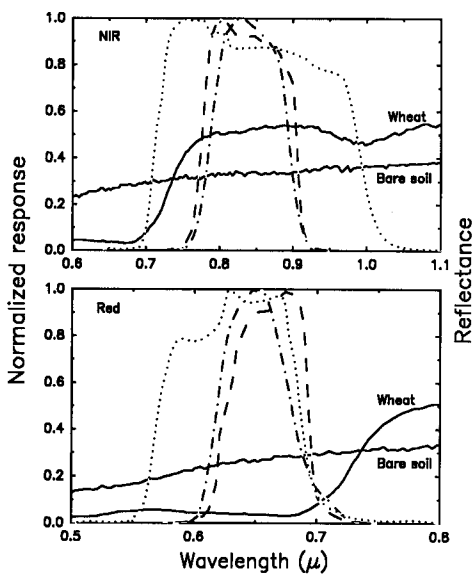

Fig. 5. Nominal red and NIR response functions for the TM (dashed lines), SPOT-HRV (dash–dot–dash lines) and the AVHRR (dotted lines). Wheat and bare soil spectra are depicted by solid lines.

TABLE 1

Reflectance values obtained by integrating the response functions and spectra in Fig. 5 (as described in the text), and the resulting VI

	LANDSAT-TM	Spot-HRV	NOAA-AVHRR
Wheat			
Red reflectance	0.040	0.041	0.047
NIR reflectance	0.517	0.519	0.471
NIR/red	12.9	12.7	10.0
NDVI	0.856	0.854	0.819
Bare soil			
Red reflectance	0.274	0.269	0.252
NIR reflectance	0.333	0.334	0.334
NIR/red	1.21	1.24	1.32
NDVI	0.097	0.108	0.134

LANDSAT-TM and SPOT-HRV, but were different for the AVHRR. The AVHRR value for the NIR/red ratio was about 22% less than that for the other two sensors. The difference was much less for bare soil. If spectra are relatively flat over a wide range of wavelengths (as is soil in Fig. 5), the response difference is small resulting in little difference between the VI. A word of caution: a comparison of VI calculated from actual satellite data would be different from the values shown in Table 1. Other factors, such as spatial resolution, sensor calibration and atmospheric effects, were not included in the theoretical example.

EFFECTS OF SOIL BACKGROUND ON VI

Until the soil is fully covered by vegetation, the soil background will influence the VI. For incomplete canopies, the wetting of a previously dry soil (or vice versa) can cause a change in VI. The change is further complicated by the fact that the transmission of light through vegetation is considerably greater in the NIR than in the red band.

Both the ratio and the linear combination (orthogonal) classes of VI rely on the existence of the soil baseline in red and NIR wavelength space for soil normalization (Huete, 1988). The intercept of this line is close to, but does not pass through, the origin (Fig. 6) and there is usually some scatter of soil points away from the principal soil line. Such secondary soil influences are most noticeable with red- and yellow-colored soils (Kauth and Thomas, 1976). These two factors affect the discrimination of low amounts of vegetation from bare soil, and are significant in arid regions and in the early stages of vegetation growth (Huete et al., 1984).

Figure 6 depicts lines of constant vegetation amounts (isolines) as pre-

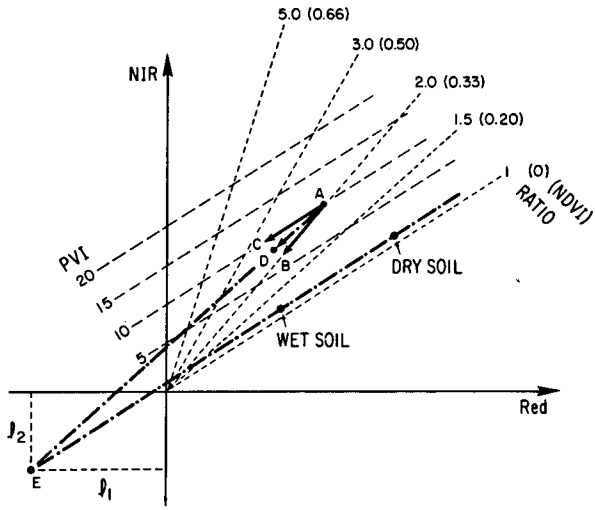

Fig. 6. Spectra isolines of equal vegetation amounts in NIR–red wavelength space as predicted by the RVI, NDVI and the PVI (adapted from Huete, 1988).

dicted by the RVI, NDVI and PVI. The ratio indices are graphically displayed by vegetation isolines of increasing slopes diverging out from the origin, while PVI isolines remain parallel to the soil line. To show soil influences on VI in partially vegetated areas, consider a pixel representing a partial canopy over a dry soil background (Point A, Fig. 6). If the soil background were to become wet, a vegetation isoline bounded by dry and wet soil conditions would be formed. In order for the ratio indices to effectively normalize such a background change, the pixel values would have to shift directly toward the origin (B), following an isoline of constant RVI or NDVI values. The PVI, however, would require the pixel values to shift along an isoline parallel to the soil line (C), so that both the wet- and dry-soil partially vegetated pixels would maintain a constant PVI value (equidistant to the soil line). As the soil darkens on wetting (Fig. 6), the actual pixel shifts to D and thus the PVI value of the partially vegetated pixel (D) with wet soil is lower than that of the dry soil (A), while the wet pixel RVI and NDVI values exceed those of the dry soil.

Huete (1988) developed a means to minimize the effect of soil background on the ratio VI. He extended the line A–D (Fig. 6) to the point of intersection with the soil line (E), and showed that by adding the distances l_1 and l_2 to the red and NIR values, respectively, the resulting ratio indices would be only minimally affected by soil background. Assuming that $l_1 = l_2$ and using the format for NDVI, Huete (1988) defined the soil-adjusted vegetation index (SAVI) as

$$\mathrm{SAVI} = \frac{\mathrm{NIR} - \mathrm{red}}{\mathrm{NIR} + \mathrm{red} + \mathrm{L}}(1 + L) \tag{10}$$

where $L = l_1 + l_2 = 2l$. The multiplicative factor $(1+L)$ was necessary to maintain the same bounds as the NDVI. Huete (1988) showed that optimal L values were different for different vegetation amounts, but concluded that $L = 0.5$ was optimal for a wide range of conditions. Although the SAVI was developed using ground-based data, Huete and Warrick (1990) demonstrated that it successfully minimized soil background effects using satellite data.

The development of improved VI is an ongoing process. Major et al. (1990) used modeled data (in contrast to Huete's experimental data) to adjust the RVI for soil background. Baret and Guyot (1991) discussed the potentials and limits of several VI for estimating leaf area index.

EFFECTS OF VIEW AND SOLAR ANGLES ON VI

Light is reflected uniformly in all directions from a lambertian surface, a condition that rarely exists in nature. Vegetated surfaces are markedly non-lambertian and light reflected from such a surface is highly dependent on view and solar angles. This can be visualized by considering a row crop (e.g. cotton) that has not reached full cover. If the rows are north–south, the soil between the rows will be shaded early and late in the day, and sunlit at midday. If an instrument views the scene from directly overhead (nadir), the red reflectance would be low in the morning and increase as the sun rises because of the increasing amount of sunlit soil. The NIR, however, would not change nearly as much because roughly half of this light is transmitted through the

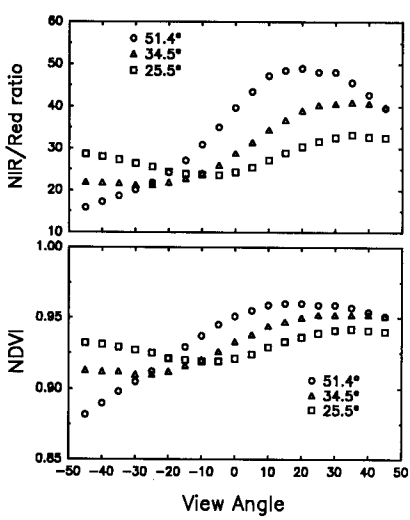

Fig. 7. Effect of view angle on the NDVI and the RVI at three solar zenith angles over a wheat canopy.

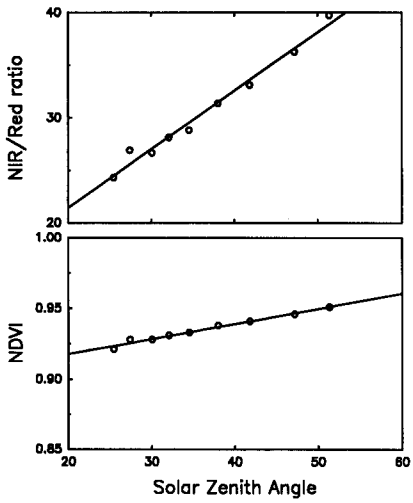

Fig. 8. Effect of solar zenith angle on the NDVI and the RVI at one view angle (nadir) over a wheat canopy.

canopy and can be reflected from the shaded soil. This explanation is greatly simplified. The actual situation is extremely complex. Nevertheless, it becomes obvious that different view and solar angles will cause different values of VI to be obtained for the same surface.

View angle and solar angle effects on radiation reflected on the surface have been discussed at length in the literature (see Pinter et al. (1983) for an extensive list of references). Their effects on VI have been reported by Pinter et al. (1983, 1987, 1990) and Jackson et al. (1979, 1990). Examples of these effects are shown in Figs. 7 and 8. Figure 7 shows changes in the NIR/red ratio and the NDVI as caused by view angle changes (for three solar angles) over a wheat canopy. At the largest solar zenith angle (51.4°), the NIR/red ratio more than doubled as view angles changed from −45° (viewing toward the sun) to +45° (viewing away from the sun), whereas the NDVI changed from about 0.88 to 0.96. Figure 8 shows changes in the two indices with changes in the solar zenith angle, at a constant view angle (nadir). Again, the NIR/red ratio nearly doubled for a sun angle change of less than 30°, and the NDVI changed from about 0.92 to 0.94 for the same range of sun angles. The NDVI appears to be less sensitive to view and solar angle changes than is the NIR/red ratio; however, the data were obtained for a high vegetation density where the NDVI is least sensitive.

ATMOSPHERIC EFFECTS ON VI

Obtaining quantitative results from satellite data requires an accurate accounting for atmospheric effects. VI are not immune to these effects. Switzer

et al. (1981) pointed out that atmospheric path radiance contributes to falsely low values of the NIR/red ratio in LANDSAT data. Dave (1980, 1981) simulated satellite data and demonstrated the effect of different atmospheres on the NIR/red ratio and the tasseled cap transformation of Kauth and Thomas (1976). Jackson et al. (1983) examined the effect of the atmosphere on a number of vegetation indices by simulating LANDSAT MSS data for a data set comprising season-long reflectance measurements over wheat. In general, both ratio and linear combination indices decrease with increasing atmospheric turbidity.

EFFECT OF CANOPY ARCHITECTURE ON VI

The architecture of a vegetation canopy determines the directions that radiation will be reflected from plant surfaces. The vertical elements of an erectophile canopy trap reflected radiation within the canopy, with a corresponding reduction in the amount reflected vertically towards a nadir-oriented radiometer. The opposite is true for a planophile canopy. The horizontal leaves reflect more in the vertical direction and less is trapped within the canopy (Suits, 1972; Bunnik, 1978). A nadir-pointing sensor can receive 20–30% more reflected radiation from a planophile canopy than from an erectophile canopy.

Canopy architectural effects on VI were examined by Jackson and Pinter (1986). They showed that during the period of peak green vegetation densities, the RVI was about 30% higher for an erectophile canopy than for a planophile canopy. On the other hand, the PVI was about 30% higher for the planophile canopy than for the erectophile canopy. Thus, within a scene that contains similar amounts of vegetation, but different geometries, different VI will respond differently to canopy architecture. At first glance, this complicating feature would diminish the value of VI. In fact, it adds a new perspective that could possibly be exploited to provide otherwise unobtainable information on canopy architectural features within a scene.

CONCLUDING REMARKS

VI are useful for assessing the amount and condition of vegetation using data from ground-, aircraft- and satellite-based sensors. However, atmospheric constraints, sensor view and solar zenith angles, as well as soil background and canopy architecture, must be accounted for if quantitative comparisons of biomass and plant health are to be expected. The effective use of VI requires that the complex interplay of all the above influences be simultaneously considered. It is important that the VI is able to respond to subtle changes in plant health status amidst variable view, illumination and atmospheric conditions.

ACKNOWLEDGMENT

We thank Paul J. Pinter, Jr. for providing the reflectance data for cotton used in Figs. 2 and 3.

REFERENCES

Baret, F. and Guyot, G., 1991. Potentials and limits of vegetation indices for LAI and APAR assessment. Remote Sensing Environ., 35: 161–173.

Bunnik, N.J.J., 1978. The Multispectral Reflectance of Shortwave Radiation by Agricultural Crops in Relation with their Morphological and Optical Properties. Veenman and Zonen, Wageningen, 175 pp.

Dave, J.V., 1980. Effect of atmospheric conditions on remote sensing of vegetation parameters. Remote Sensing Environ., 10: 87–99.

Dave, J.V., 1981. Influence of illumination and viewing geometry and atmospheric composition of the "tasseled cap" transformation of Landsat MSS data. Remote Sensing Environ., 11: 37–55.

Deering, D.W., 1978. Rangeland reflectance characteristics measured by aircraft and spacecraft sensors. Ph.D. Dissertation, Texas A & M University, College Station, TX, 338 pp.

Freiberger, W.F. (Editor), 1960. The International Dictionary of Applied Mathematics. Van Nostrand, Princeton, NJ, p. 412.

Huete, A.R., 1988. A soil-adjusted vegetation index (SAVI). Remote Sensing Environ., 25: 295–309.

Huete, A.R. and Warrick, A.W., 1990. Assessment of vegetation and soil water regimes in partial canopies with optical remotely sensed data. Remote Sensing Environ., 32: 155–167.

Huete, A.R., Post, D.F. and Jackson, R.D., 1984. Soil spectral effects on 4-space vegetation discrimination. Remote Sensing Environ., 15: 155–165.

Jackson, R.D., 1983. Spectral indices in n-space. Remote Sensing Environ., 13: 409–421.

Jackson, R.D. and Pinter, Jr., P.J., 1986. Spectral response of architecturally different wheat canopies. Remote Sensing Environ., 20: 43–56.

Jackson, R.D., Pinter, Jr., P.J., Idso, S.B. and Reginato, R.J., 1979. Wheat spectral reflectance: interactions between crop configuration, sun elevation, and azimuth angle. Appl. Optics, 18: 3730–3732.

Jackson, R.D., Pinter, Jr., P.J., Reginato, R.J. and Idso, S.B., 1980. Hand-held radiometry. USDA-SEA-AR Agricultural Reviews and Manuals, US Department of Agriculture, Oakland, CA, W-19, 66 pp.

Jackson, R.D., Slater, P.N. and Pinter, Jr., P.J., 1983. Discrimination of growth and water stress in wheat by various vegetation indices through clear and turbid atmospheres. Remote Sensing Environ., 13: 187–208.

Jackson, R.D., Teillet, P.M., Slater, P.N., Fedosejevs, G., Jasinski, M.F., Aase, J.K. and Moran, M.S., 1990. Bidirectional measurements of surface reflectance for view angle corrections of oblique imagery. Remote Sensing Environ., 32: 189–202.

Jordan, C.F., 1969. Derivation of leaf area index from quality of light on the forest floor. Ecology, 50: 663–666.

Kauth, R.J. and Thomas, G.S., 1976. The tasseled cap—A graphic description of the spectral-temporal development of agricultural crops as seen by Landsat. Proceedings of Symposium on Machine Processing of Remotely Sensed Data, Purdue University, West Lafayette, IN, pp. 41–51.

Kauth, R.J., Lambeck, P.F., Richardson, W., Thomas, G.S. and Pentland, A.P., 1979. Feature

extraction applied to agricultural crops as seen by Landsat. Proceedings of LACIE Symposium, NASA/Johnson Space Center, Houston, TX, pp. 705–721.

Lambeck, P.F., Kauth, R.J. and Thomas, G.S., 1978. Data screening and preprocessing for Landsat MSS data. Proceedings of 12th International Symposium on Remote Sensing of Environment, ERIM, Ann Arbor, MI, pp. 999–1008.

Major, D.J., Baret, F. and Guyot, G., 1990. A ratio vegetation index adjusted for soil brightness. Int. J. Remote Sensing, 11: 727–740.

Moran, M.S., Jackson, R.D., Hart, G.F., Slater, P.N., Bartell, R.J., Biggar, S.F., Gellman, D.I. and Santer, R.P., 1990. Obtaining surface reflectance factors from atmospheric and view angle corrected SPOT-1 HRV data. Remote Sensing Environ., 32: 203–214.

Perry, C.R. and Lautenschlager, L.F., 1984. Functional equivalence of spectral vegetation indices. Remote Sensing Environ., 14: 169–182.

Pinter, Jr., P.J., Jackson, R.D., Idso, S.B. and Reginato, R.J., 1983. Diurnal patterns of wheat spectral reflectances. IEEE Trans. Geosci. Remote Sensing, GE-21: 156–163.

Pinter, Jr., P.J., Zipoli, G., Maracchi, G. and Reginato, R.J., 1987. Influence of topography and sensor view angles on NIR/red ratio and greenness vegetation indices of wheat. Int. J. Remote Sensing, 8: 953–957.

Pinter, Jr., P.J., Jackson, R.D. and Moran, M.S., 1990. Bidirectional reflectance factors of agricultural targets: A comparison of ground-, aircraft-, and satellite-based observations. Remote Sensing Environ., 32: 215–228.

Price, J.C., 1987. Calibration of satellite radiometers and the comparison of vegetation indices. Remote Sensing Environ., 21: 15–27.

Richardson, A.J. and Wiegand, C.L., 1977. Distinguishing vegetation from soil background information. Photogramm. Eng. Remote Sensing, 43: 1541–1552.

Slater, P.N., 1980. Remote Sensing: Optics and Optical Systems. Addison-Wesley, Reading, MA, 575 pp.

Suits, G.H., 1972. The calculation of the directional reflectance of a vegetative canopy. Remote Sensing Environ., 2: 117–125.

Switzer, P., Kowalik, W.S. and Lyon, R.J.P., 1981. Estimation of atmospheric path-radiance by the covariance matrix method. Photogramm. Eng. Remote Sensing, 47: 1469–1476.

Tucker, C.J., 1979. Red and photographic infrared linear combinations for monitoring vegetation. Remote Sensing Environ., 8: 127–150.